4A2 Computational Fluid Dynamics - Interim Report

5690G

1 Euler Solver

1.1 Test Case 0

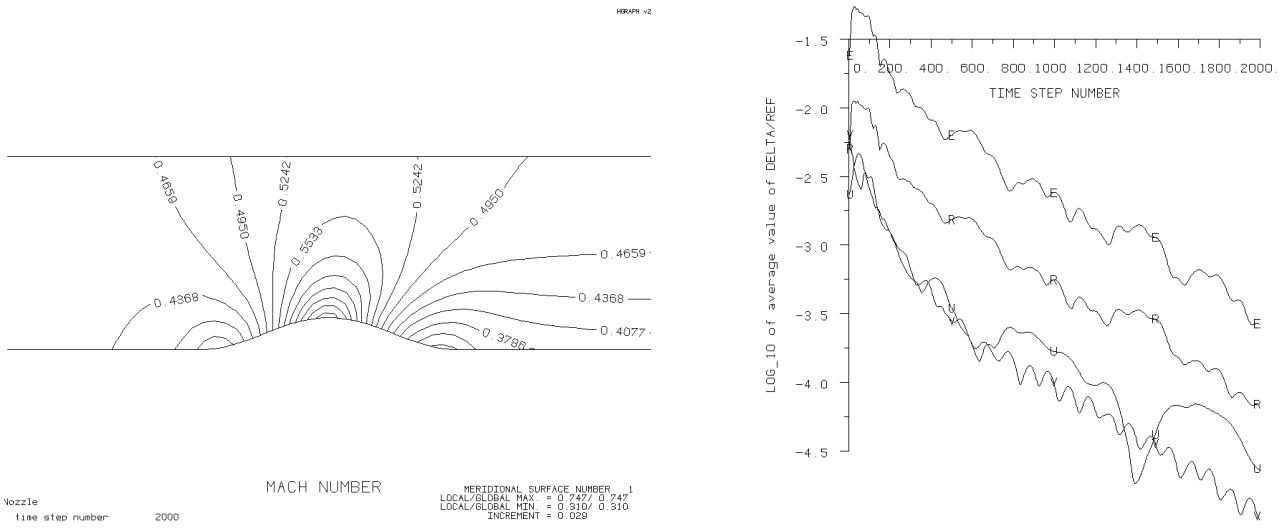

(a) Mach number contours.

(b) Log plot of convergence against time steps.

Figure 1: Test Case 0

Test case 0 simulates a nozzle with a contraction and then expansion of a pipe. The inlet flow is subsonic and hence the velocity of the flow increases at the contraction as the area decreases (see Figure 1a). For an inviscid flow, the contour lines of mach number should be symmetric about the center of the contraction. Figure 1a shows that this is not the case in the solution found. This is because artificial viscosity is introduced through the smoothing step of the method. This step is required to maintain the stability of the Lax method because the central difference scheme (see Figure 3 for code) used is inherently unstable. The viscous losses are visualised in the contour plot of stagnation pressure (Figure 2). Viscous losses result in a decrease in stagnation pressure and hence regions of high loss can be identified by reduced stagnation pressure. This shows that the viscous losses mostly occur downstream of the contraction as expected since this is where velocity gradients normal to the flow are largest.

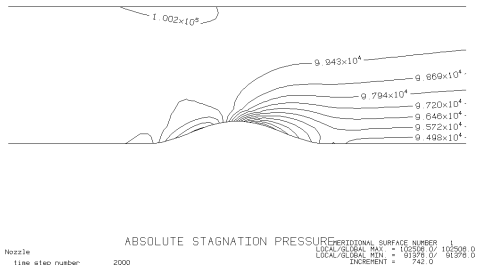

Figure 2: Stagnation pressure contours for test case 0.

Figure 1a also shows the mach number of the flow increases at the contraction of the pipe. This was expected since the flow area decreases and so the flow velocity must increase in order for mass to be conserved. Additionally, the solution shows that the flow at the top of the pipe at exit has a higher mach number than the flow at the bottom. Figure 1b shows that the flow parameters follow a relatively linear trend to convergence on the logarithmic plot.

```
do i=2,ni-1
  do j=2,nj-1
    prop_inc(i,j) = 0.25*(delprop(i,j) + delprop(i-1,j) + delprop(i,j-1) + delprop(i-1,j-1))
  enddo
enddo
```

Figure 3: Central difference method code used to find the increment of each node.

1.2 Test Case 1

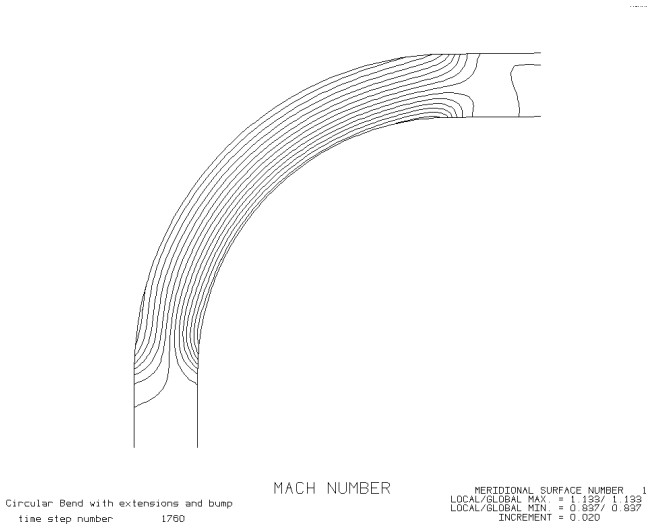

(a) Mach number contours.

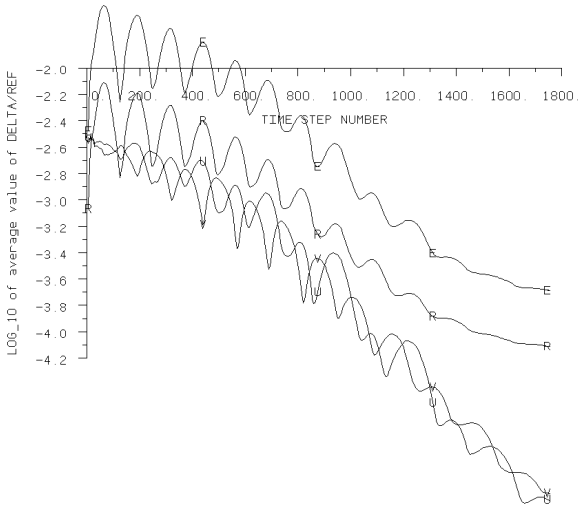

(b) Log plot of convergence against time steps.

Figure 4: Test Case 1

Test case 1 consists of a circular bend with extensions. The contour plot (Figure 4a) shows that there is a large velocity gradient radially across the bend with many contour lines tangential to the radius of the circular bend. The inlet flow condition is subsonic, however, the maximum mach contour is 1.133 and the minimum is 0.837. In the solution, as shown in Figure 4a, the flow around the outside of the bend is supersonic and the flow around the inside of the bend remains subsonic. This is an interesting feature of the solution and suggests there may be more complicated flow features arising under these conditions than the solution suggests. Additionally, the central difference scheme used in the Lax method is unsuitable in the supersonic flow region because information can't propagate upstream under supersonic conditions.

Figure 4b shows the convergence of the flow parameters against time steps. Interestingly this test case converges more rapidly than in test case 0. This could be because the flow area is constant and so the initial guess is more accurate. Additionally, the convergence of the flow parameters is more oscillatory and the parameter U and V appear to oscillate in anti-phase to one another.

Viscous losses are also present in this solution. This is visualised in the contour plot of stagnation pressure (Figure 5). This plot shows that stagnation pressure losses occur along the circular pipe particularly at the walls of the inlet and exit of the bend. Viscous losses occur where there is a velocity gradient normal to the flow direction and as discussed in Figure 4a there are large velocity gradients normal to the flow direction around the bend in the pipe. These losses would not be present in an inviscid flow and are introduced by the smoothing step of the method.

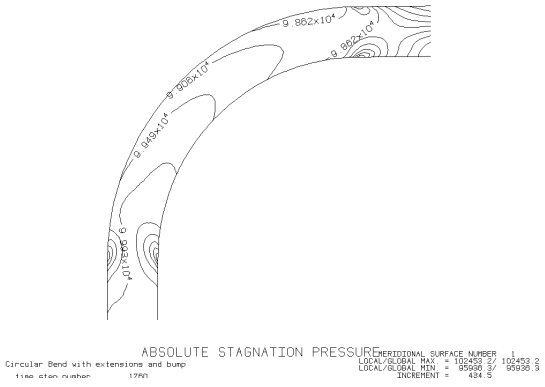

Figure 5: Stagnation pressure contours for test case 1.

2 Advection

The linear convection equation used in all of the following finite difference schemes is:

$$\frac{\partial u}{\partial t} + a\frac{\partial u}{\partial x} = 0 \tag{1}$$

2.1 Upwind Difference Scheme

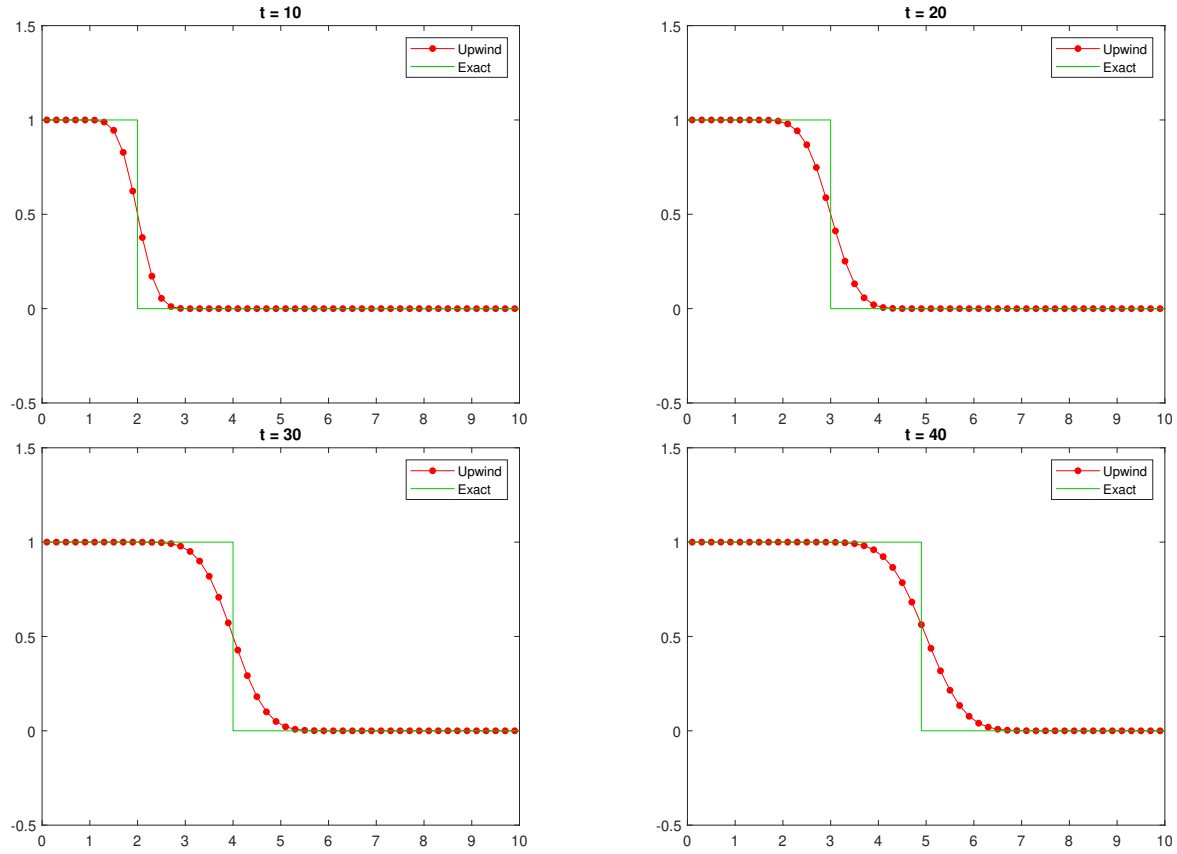

Figure 6: Upwind difference scheme against exact solution at various time steps.

The value at position i and time $n+1$ is calculated according to Equation 2

$$u_i^{n+1} = u_i^n - a\frac{\Delta t}{\Delta x}(u_i^n - u_{i-1}^n) \tag{2}$$

Using the Taylor series expansions for u_i^{n+1} and u_i^n (Equations 3a and 3b respectively) the modified linear convection equation can be reached (Equation 4).

$$u_i^{n+1} = u_i^n + \Delta t\frac{\partial u}{\partial t}\Big|_i^n + \frac{\Delta t^2}{2}\frac{\partial^2 u}{\partial t^2}\Big|_i^n + \ldots \tag{3a}$$

$$u_{i+1}^n = u_i^n + \Delta x\frac{\partial u}{\partial x}\Big|_i^n + \frac{\Delta x^2}{2}\frac{\partial^2 u}{\partial x^2}\Big|_i^n + \frac{\Delta x^3}{6}\frac{\partial^3 u}{\partial x^3}\Big|_i^n + \ldots \tag{3b}$$

$$\frac{\partial u}{\partial t} + a\frac{\partial u}{\partial x} = D\frac{\partial^2 u}{\partial x^2} + O(\Delta t^2, \Delta x^2) \tag{4}$$

Where,

$$D = \frac{a\Delta x}{2}\Big(1 - \Big(\frac{\Delta t}{\Delta x}a\Big)\Big)$$

Equation 4 shows that this scheme is first order accurate in space and time. The term $D\frac{\partial^2 u}{\partial x^2}$ represents artificial diffusion, introduced by the numerical scheme. For stability, D must be positive in order to damp out oscillations.

Therefore, the term $\frac{\Delta t}{\Delta x}a$ must be less than 1 for stability. The diffusion of the solution is shown clearly in Figure 6; as the time increases the discontinuity becomes spread out over an increasing number of points. The upwind scheme produces a similar solution to the TVD method shown in Section 2.5 but the shape of the discontinuity is not as well preserved.

2.2 Central Difference Scheme

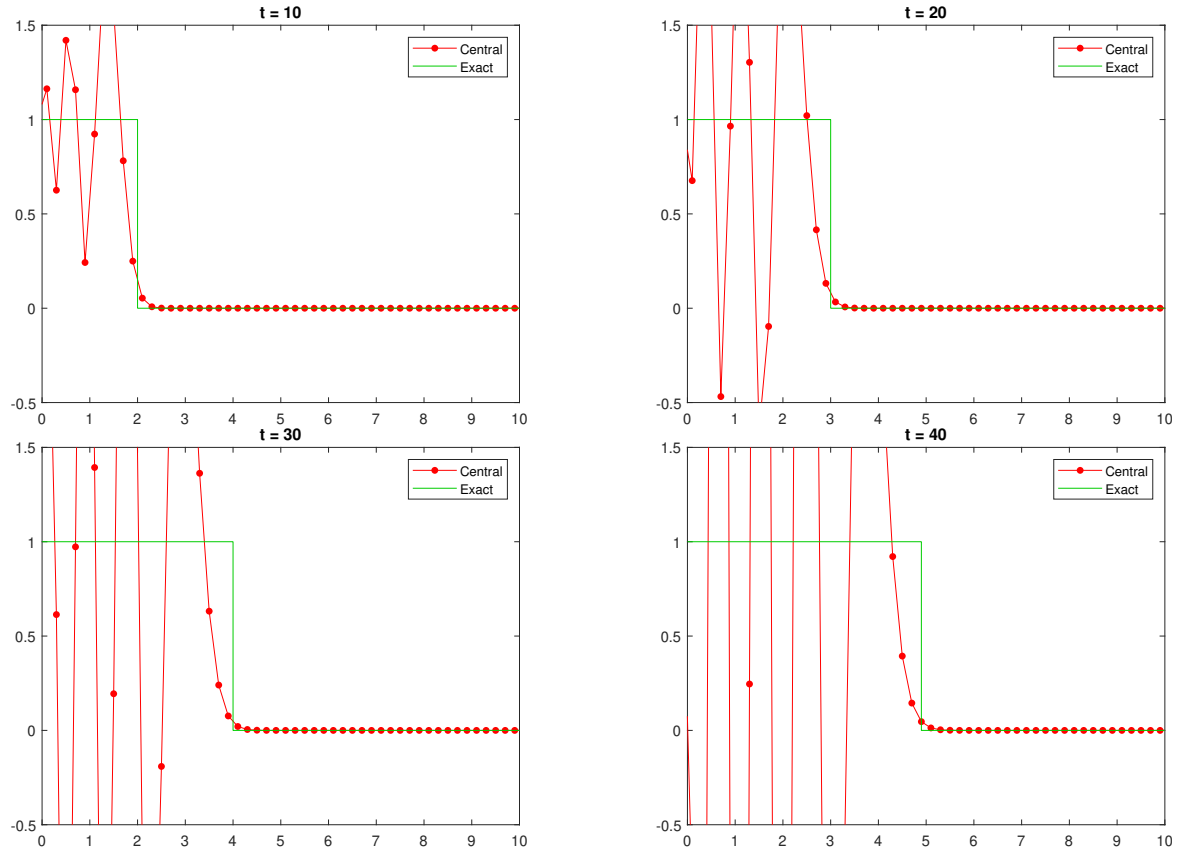

Figure 7: Central difference scheme against exact solution at various time steps.

Using the central difference scheme, the value at position i and time $n+1$ is calculated with Equation 5.

$$u_i^{n+1} = u_i^n - a\frac{\Delta t}{2\Delta x}(u_{i+1}^n - u_{i-1}^n) \tag{5}$$

In a similar way to the upwind scheme, the Taylor series expansions (Equations 6a-6c) can be used to arrive at the modified equation for the linear convection equation using the central difference scheme (Equation 7).

$$u_i^{n+1} = u_i^n + \Delta t\frac{\partial u}{\partial t}\Big|_i^n + \frac{\Delta t^2}{2}\frac{\partial^2 u}{\partial t^2}\Big|_i^n + \ldots \tag{6a}$$

$$u_{i+1}^n = u_i^n + \Delta x\frac{\partial u}{\partial x}\Big|_i^n + \frac{\Delta x^2}{2}\frac{\partial^2 u}{\partial x^2}\Big|_i^n + \frac{\Delta x^3}{6}\frac{\partial^3 u}{\partial x^3}\Big|_i^n + \ldots \tag{6b}$$

$$u_{i-1}^n = u_i^n - \Delta x\frac{\partial u}{\partial x}\Big|_i^n + \frac{\Delta x^2}{2}\frac{\partial^2 u}{\partial x^2}\Big|_i^n - \frac{\Delta x^3}{6}\frac{\partial^3 u}{\partial x^3}\Big|_i^n + \ldots \tag{6c}$$

$$\frac{\partial u}{\partial t} + a\frac{\partial u}{\partial x} = -\frac{\Delta t}{2}\frac{\partial^2 u}{\partial t^2}\Big|_i^n - \frac{\Delta x^2}{6}a\frac{\partial^3 u}{\partial x^3}\Big|_i^n + O(\Delta t^2, \Delta x^4) \tag{7}$$

Equation 7 shows that the central difference scheme is first order accurate in time and second order accurate in space. However, using the linear convection equation (Equation 1) it can be shown that:

$$\frac{\partial^2 u}{\partial t^2}\Big|_i^n = a^2\frac{\partial^2 u}{\partial x^2}\Big|_i^n \tag{8}$$

Therefore Equation 7 can be rewritten as:

$$\frac{\partial u}{\partial t} + a\frac{\partial u}{\partial x} = -a^2\frac{\Delta t}{2}\frac{\partial^2 u}{\partial x^2}\Big|_i^n - \frac{\Delta x^2}{6}a\frac{\partial^3 u}{\partial x^3}\Big|_i^n + O(\Delta t^2, \Delta x^4) \tag{9}$$

The term $-a^2\frac{\Delta t}{2}\frac{\partial^2 u}{\partial x^2}\Big|_i^n$ is a viscosity term with coefficient of viscosity $-a^2\frac{\Delta t}{2}$. This term is always negative and hence the scheme is unstable because a negative viscosity amplifies any disturbances. This can be seen clearly in Figure 7 as the solution rapidly diverges from the exact solution. The solution downstream of the discontinuity is unstable and the solution is significantly worse than that of the TVD method shown in Section 2.5.

2.3 Lax-Wendroff

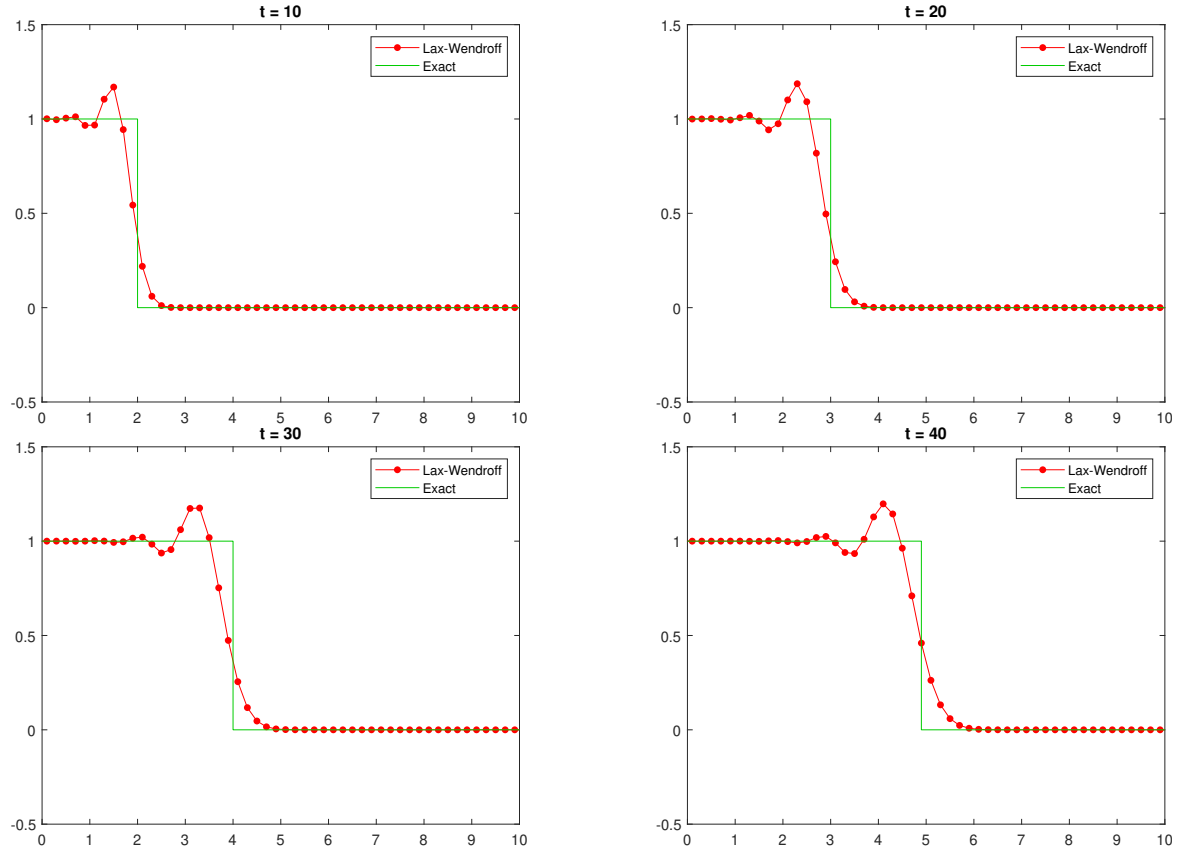

Figure 8: Lax-Wendroff method against exact solution at various time steps.

Using the Lax-Wendroff method, the value at position i and time $n+1$ can be calculated using Equation 10.

$$u_i^{n+1} = u_i^n - a\frac{\Delta t}{2}(u_{i+1}^n - u_{i-1}^n) + a^2\frac{\Delta t^2}{2\Delta x^2}(u_{i+1}^n - 2u_i^n + u_{i-1}^n) \tag{10}$$

Again, using the Taylor series expansions and the relation shown in Equation 8, the modified linear convection equation can be written as:

$$\frac{\partial u}{\partial t} + a\frac{\partial u}{\partial x} = \mu\frac{\partial^3 u}{\partial x^3} + O(\Delta t^4, \Delta x^4) \tag{11}$$

Where,

$$\mu = \frac{\Delta x^2}{6}a\Big(\frac{\Delta t^2}{\Delta x^2}a^2 - 1\Big)$$

This scheme is second order accurate in space and time (see Equation 11). The term $\mu\frac{\partial^3 u}{\partial x^3}$ is a dispersive term. It can be shown that the group velocity can be calculated as a function of wavenumber using to Equation 12.

$$c_g(k) = a + 3\mu k^2 \tag{12}$$

Where k is the wavenumber.

Since $a > 0$ and $\left|\frac{\Delta t}{\Delta x}a\right| < 1$ for stability, $\mu < 0$. Therefore, all wavenumbers travel slower than the linear convection velocity ('a'). Since the discontinuity in the initial data has a wide Fourier spectrum, this leads to an oscillatory wave train lagging behind the discontinuity of the exact solution. This is seen clearly in Figure 8; where the oscillations increase in amplitude and fall further behind the discontinuity in the exact solution as the time increases. The gradient around the discontinuity is maintained far better than in the upwind method, however the oscillations behind the discontinuity are unphysical. These oscillations are not seen in the higher order TVD method.

2.4 Beam-Warming

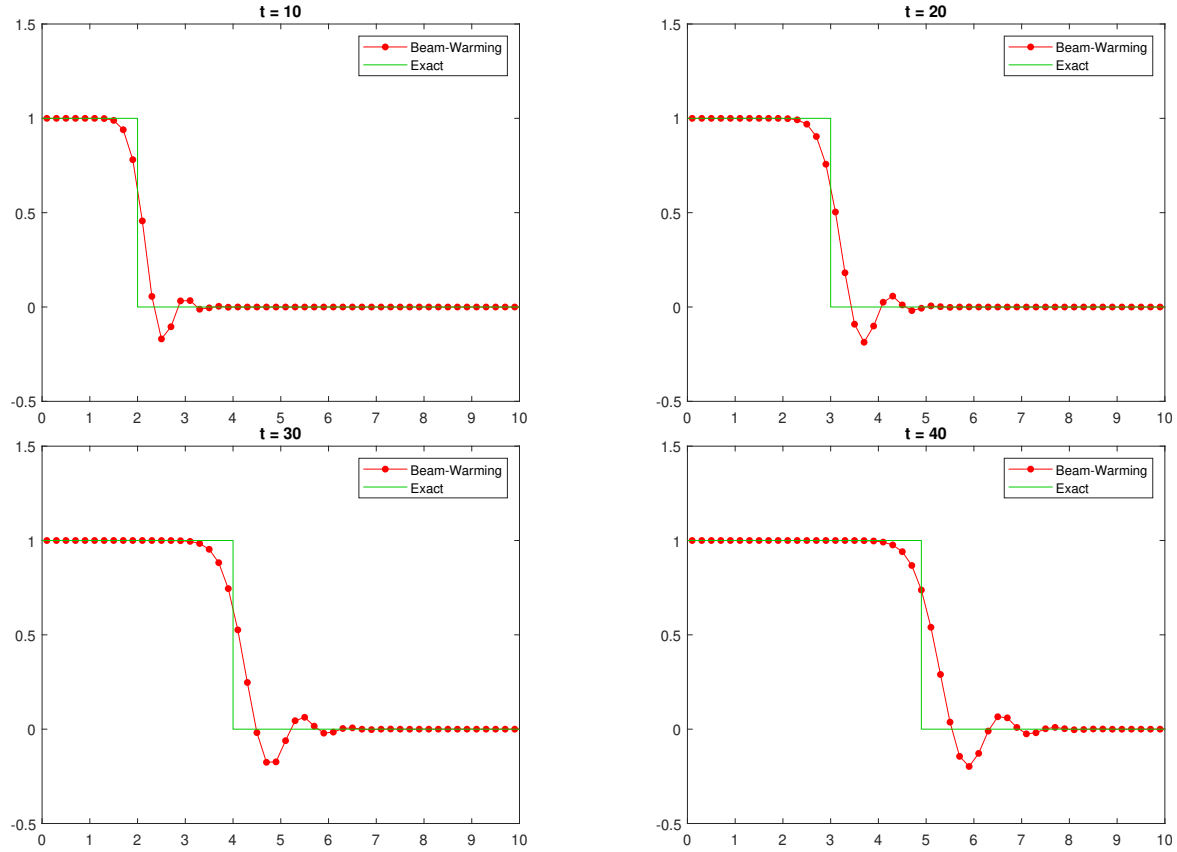

Figure 9: Beam-Warming method against exact solution at various time steps.

The beam-warming method is similar to the Lax-Wendroff method. However, instead of centered finite difference approximations, the beam-warming method uses upwind points. These approximations are shown in Equations 13a and 13b and are used to calculate the value at position i and time $n+1$ according to Equation 14.

$$\left.\frac{\partial u}{\partial x}\right|_i^n \approx \frac{1}{\Delta x}(3u_i^n - 4u_{i-1}^n + u_{i-2}^n) \tag{13a}$$

$$\left.\frac{\partial^2 u}{\partial x^2}\right|_i^n \approx \frac{1}{\Delta x^2}(u_i^n - 2u_{i-1}^n + u_{i-2}^n) \tag{13b}$$

$$u_i^{n+1} = u_i^n - a\frac{\Delta t}{2}(3u_i^n - 4u_{i-1}^n + u_{i-2}^n) + a^2\frac{\Delta t^2}{2\Delta x^2}(u_i^n - 2u_{i-1}^n + u_{i-2}^n) \tag{14}$$

The modified linear convection equation for this scheme is very similar to the Lax-Wendroff scheme except the dispersion constant is different.

$$\frac{\partial u}{\partial t} + a\frac{\partial u}{\partial x} = \mu\frac{\partial^3 u}{\partial x^3} + O(\Delta t^4, \Delta x^4) \tag{15}$$

Where,

$$\mu = \frac{\Delta x^2}{6} a \Big(\frac{\Delta t^2}{\Delta x^2} a^2 - 3 \frac{\Delta t}{\Delta x} a + 2 \Big)$$

Equation 15 shows that this method is second order accurate in space and time. The group velocity for this method is calculated according to Equation 12. For $0 < \frac{\Delta t}{\Delta x} a < 1$, $\mu > 0$ and so the oscillations travel ahead of the discontinuity. This is observed clearly in Figure 9 ($\frac{\Delta t}{\Delta x} a = 0.8$) with the oscillations increasing in amplitude and moving further ahead of the discontinuity in the exact solution as the time increases. If $1 < \frac{\Delta t}{\Delta x} a < 2$, then $\mu < 0$ and the oscillations would fall behind the discontinuity in a similar way to the Lax-Wendroff method. The gradient of the discontinuity is better maintained than in the upwind scheme. However, the oscillations observed in the solution are not physical and are not seen in the higher order TVD method.

2.5 TVD method with superbee limiter

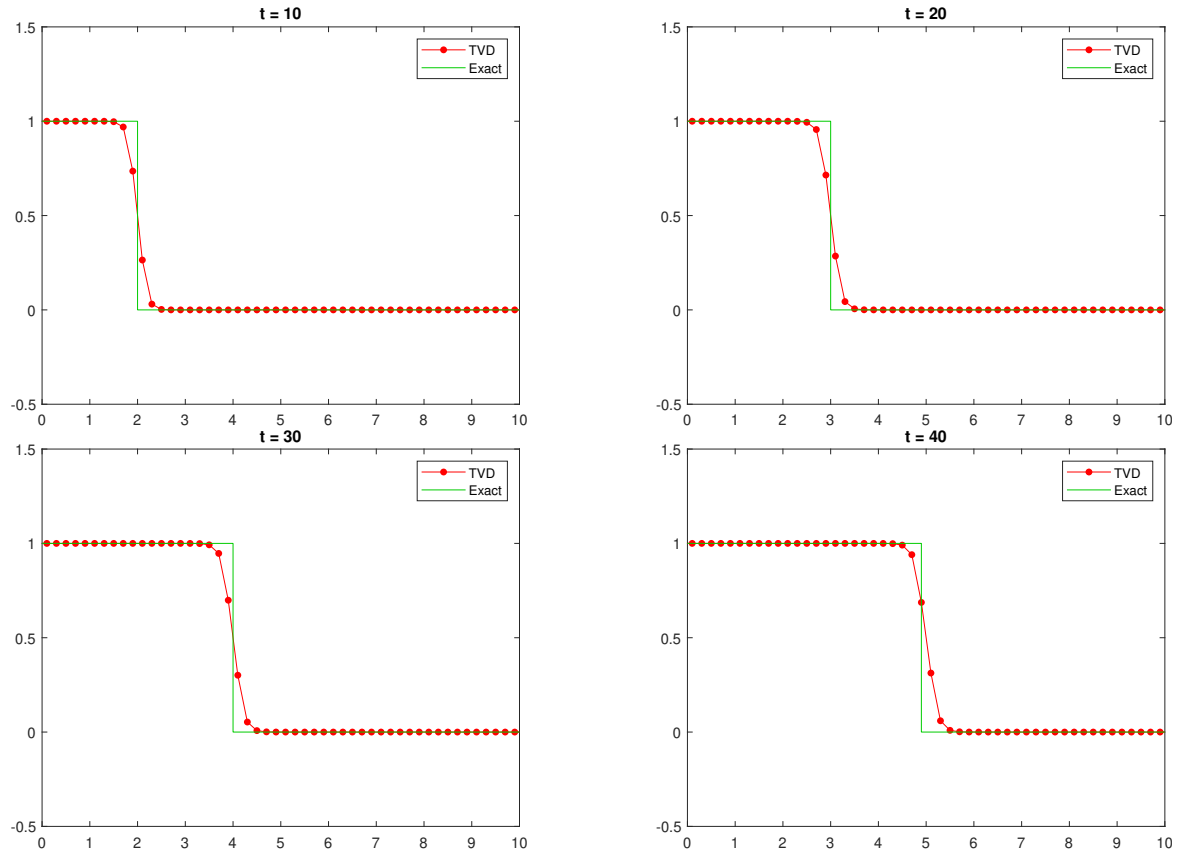

Figure 10: TVD method against exact solution at various time steps.

Figure 10 shows that the TVD method with the superbee limiter is considerably more accurate than the previous schemes. It is able to maintain the shape of the discontinuity relatively well (similar to the Lax-Wendroff and Beam-Warming methods). However, the scheme is not susceptible to oscillations, similar to the upwind method.